

Schmidt, *ibid.*, p. 64.

<sup>2</sup>B. Feuerbacher and R. Willis, Phys. Rev. Lett. **36**, 1339 (1976), and private communication.

<sup>3</sup>W. F. Egelhoff and D. L. Perry, Phys. Rev. Lett. **34**, 93 (1975).

<sup>4</sup>P. J. Estrup and J. Anderson, J. Chem. Phys. **45**, 2254 (1966); H. Froitzheim, H. Ibach, and S. Lewald, Phys. Rev. Lett. **36**, 1549 (1976).

<sup>5</sup>D. G. Dempsey, L. Kleinman, and E. Carruthers, Phys. Rev. B **12**, 2932 (1976).

<sup>6</sup>B. Chakraborty, W. E. Pickett, and P. B. Allen, Phys. Rev. B **14**, 3227 (1976), and Phys. Lett. **48A**, 91

(1974), and private communications.

<sup>7</sup>B. Feuerbacher and B. Fitton, Phys. Rev. Lett. **30**, 923 (1973), and Phys. Rev. B **8**, 4890 (1973).

<sup>8</sup>R. F. Willis, B. Feuerbacher, and B. Fitton, Solid State Commun. **18**, 1315 (1976).

<sup>9</sup>K. Sturm and R. Feder, Solid State Commun. **14**, 1317 (1974); R. Feder and K. Sturm, Phys. Rev. B **12**, 537 (1975).

<sup>10</sup>N. Nicolaou and A. Modinos, Phys. Rev. B **11**, 3687 (1975).

<sup>11</sup>L. W. Anders, R. S. Hansen, and L. S. Bartell, J. Chem. Phys. **59**, 5277 (1973).

## Orientation of CO on Pt(111) and Ni(111) Surfaces from Angle-Resolved Photoemission\*

G. Apai, P. S. Wehner, R. S. Williams, J. Stöhr, and D. A. Shirley

*Materials and Molecular Research Division, Lawrence Berkeley Laboratory, and Department of Chemistry, University of California, Berkeley, California 94720*

(Received 28 June 1976)

Angle-resolved photoemission spectra of the molecular orbitals of chemisorbed CO on Pt(111) and Ni(111) substrates show a strong angular variation of the peak intensity ratio. Comparison with Davenport's  $X\alpha$  calculations establishes that CO stands up on these substrates, with the carbon atom bonded to the substrate. The Pt  $5d(t_{2g})$  orbitals are found to be strongly involved in chemisorption bonding to CO.

The interaction of chemisorbed adsorbate molecules with catalytically active substrates has formed the focus of much recent research activity in surface physics. Because of the importance of the CO/Pt and CO/Ni systems in heterogeneous catalysis for synthesis of hydrocarbons, these systems have served as prototypes for surface studies. Until now, however, no firm evidence has been presented regarding the orientation of adsorbate CO molecules on crystalline nickel or platinum surfaces.

Davenport<sup>1</sup> presented SW  $X\alpha$  calculations of photoelectron angular distributions from the molecular orbitals of oriented CO molecules and pointed out that chemisorbed CO should display similar angular distributions provided that the molecular wave functions are not strongly perturbed by the substrate. In this Letter, we report photoelectron angular distributions from CO adsorbed on both Pt(111) and Ni(111) surfaces. These data provide the first definitive evidence that the CO molecules "stand up" in both cases, with the carbon atoms bonded to the substrate. Furthermore, the spectra clearly show that the  $t_{2g}$  orbitals of the Pt  $5d$  band are strongly involved in the Pt-C chemisorption bond. The experiments reported here were carried out with conventional photoemission equipment (He lamp, cylindrical mirror analyzer) and thus point out the potential of such studies to determine bonding geometries. It is

clear that by making use of variable-energy, highly polarized synchrotron radiation, such studies become even more powerful.

Experiments were carried out using the  $h\nu = 40.8$  eV radiation emitted by a He II resonance lamp. Single crystals of Pt and Ni were cut along the (111) planes and cleaned *in situ* under ultra-high-vacuum conditions. In the case of Pt, it was necessary to alternate periods of Ar<sup>+</sup> bombardment of the specimen at 950°C and oxidation in an atmosphere of  $10^{-5}$  Torr O<sub>2</sub> at 850°C for two weeks in order to remove calcium and carbon impurities diffusing to the crystal surface from the bulk. Nickel was cleaned by repeated Ar<sup>+</sup> bombardment and annealing. The photoemission studies were conducted at a background pressure of impurities (other than He) less than  $8 \times 10^{-11}$  Torr. In the angle-dependent studies, both the unpolarized photon beam and the propagation direction of the analyzed electrons were in a horizontal plane, and the crystal could be rotated about a vertical axis in the plane of the (111) surface. Angle-resolved photoemission (ARP) was facilitated by masking all but an 11° arc of a cylindrical mirror analyzer, yielding an effective angular resolution of  $(5 \pm 1)^\circ$  half-angle.<sup>2</sup> Figure 1 shows the variation of the clean valence-band spectra (solid line) and the corresponding spectra after adsorption of ~4 L CO (dotted line), plotted against  $\theta$ , the angle of rotation from the

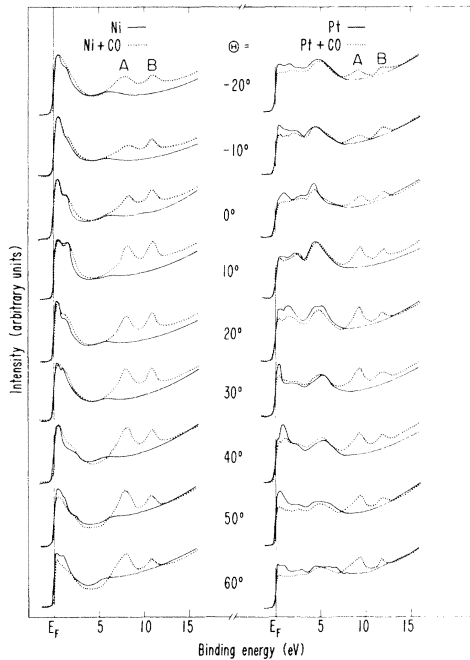


FIG. 1. Photoemission spectra of clean Ni(111) and Pt(111) (solid lines) and Ni(111) + 4 L CO and Pt(111) + 4 L CO (dotted lines) at  $h\nu = 40.8$  eV as a function of the angle  $\theta$  between the surface normal and the photoelectron propagation direction.  $\theta$  is defined in Fig. 2(a).

crystal normal to the photoelectron  $\vec{k}$  direction, for both crystals. The spectra shown in Fig. 1 were recorded with an experimental resolution of  $\sim 0.2$  eV.

The CO molecular orbitals labeled A and B in Fig. 1 are manifest as two peaks falling at  $\sim 8.1$ - and  $\sim 10.8$ -eV binding energy below the Fermi level ( $E_F$ ) in Ni and at  $\sim 9.2$  and  $\sim 11.7$  eV in Pt, respectively. The higher-binding-energy ( $E_B$ ) peak (B) has been assigned to the  $4\sigma$  orbital of CO, while the lower- $E_B$  peak (A) is attributed to a combination of the  $1\pi$  and  $5\sigma$  orbitals.<sup>3</sup> In both cases, the two peaks are of nearly equal intensity for  $\vec{k}$  near the surface normal, with the  $B/A$  ratio decreasing as  $\vec{k}$  is rotated toward the crystal surface. In Fig. 2(c) we have plotted the intensity ratio  $I_B/I_A$  of the two molecular orbitals A and B for the case of CO on Ni(111) and CO on Pt(111) as a function of the angle ( $\theta$ ) between the surface normal and photoelectron propagation direction. The details of the crystalline orientation with respect to the photon beam and the detector are shown in Figs. 2(a) and 2(b). In Fig. 2(d) we have plotted the angular dependence of the ratio  $4\sigma/(1\pi + 5\sigma)$  calculated from Davenport's angular distributions, for three orientations of the CO molecule with re-

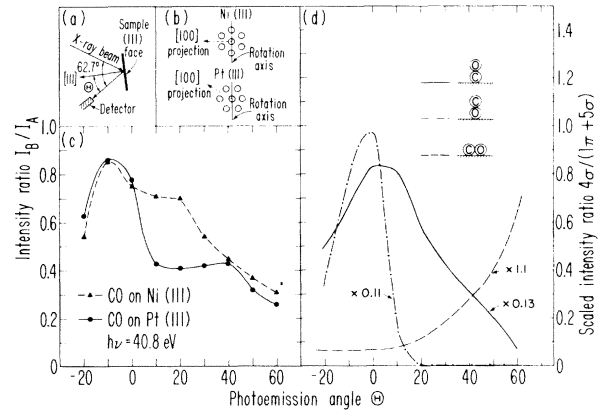


FIG. 2. (a) Experimental arrangement of the photon beam and detector with respect to the crystal normal.  $\theta$  is defined positive for clockwise rotation, negative for counterclockwise rotation of the crystal normal with respect to the fixed photoelectron propagation direction into the analyzer. (b) Experimental orientation of the crystals in the (111) plane. (c) Intensity ratio  $I_B/I_A$  of the two molecular orbital peaks A and B in Fig. 1 as a function of  $\theta$ , where  $\theta$  is defined in (a). (d) Calculated intensity ratio  $4\sigma/(1\pi + 5\sigma)$ , scaled for best fit to experiment, for three orientations of the CO molecule with respect to the surface as a function of  $\theta$ , where  $\theta$  is defined in (a).

spect to the surface. The calculations have been scaled for the best fit to the experimental curves. We believe that this is justified because Davenport's calculation does not predict the correct magnitude for the total cross section of the  $1\pi$  and the  $4\sigma$  orbitals at  $h\nu \approx 41$  eV (see Fig. 2, Ref. 1). For this reason we compare our results only to the angular dependence of the ratio and not the absolute magnitude.

In our calculation, we take the unpolarized incident radiation to be composed of two orthogonal linearly polarized components one of which is in the plane containing the incoming photon beam and the detector and the other is perpendicular to this plane ( $\vec{A} = \vec{A}_{\parallel} + \vec{A}_{\perp}$ ). Since for unpolarized light the two components  $\vec{A}_{\parallel}$  and  $\vec{A}_{\perp}$  are incoherent, the photoexcitation matrix element can be written

$$\int_0^{2\pi} \langle f | \vec{A} \cdot \vec{p} | i \rangle^2 d\alpha \sim \langle f | \vec{A}_{\parallel} \cdot \vec{p} | i \rangle^2 + \langle f | \vec{A}_{\perp} \cdot \vec{p} | i \rangle^2. \quad (1)$$

The contributions from the two components to the differential photoemission cross section were calculated according to the following analytical ex-

pression,<sup>4</sup>

$$d\sigma/d\Omega = A(\theta) \cos^2\theta_A + [B(\theta) + C(\theta) \cos 2\varphi] \\ \times \sin^2\theta_A + D(\theta) \sin\varphi \sin\theta_A \cos\theta_A, \quad (2)$$

where  $\theta_A$  is the polar angle of  $\vec{A}_{\parallel}$  or  $\vec{A}_{\perp}$ , respectively, and  $\theta$  and  $\varphi$  are the usual polar and azimuthal angles of photoemission with respect to the CO axis of the oriented molecule.<sup>1</sup>

Comparison of the experimental intensity ratio  $I_B/I_A$  for the adsorbate-substrate systems [ Fig. 2(c) ] with the scaled theoretical intensity ratio  $4\sigma/(1\pi + 5\sigma)$  for an oriented CO molecule [ Fig. 2(d) ] strongly favors the configuration where CO stands up, with the C bonded to the substrate. Note in particular that the configuration with O bonded to the substrate can be excluded because the  $4\sigma/(1\pi + 5\sigma)$  ratio vanishes for angles  $\theta \geq 20^\circ$ . The overall good agreement between the experimental curves in Fig. 2(c) and the solid curve in Fig. 2(d) is not expected to be perfect in detail, mainly because the  $5\sigma$  orbital is expected to be somewhat perturbed through its interaction with the substrate.<sup>5</sup> We feel that the present results, besides determining the orientation of CO on Ni(111) and Pt(111), also prove in general that angle-resolved ultraviolet photoemission can be used to determine bonding geometries. One other point which needs to be discussed is the difference in behavior of the ratio  $I_B/I_A$  with  $\theta$  for CO on Ni(111) and for CO on Pt(111). This may be due to a difference in the detailed nature of the adsorbate-substrate bonding for the two systems resulting in initial<sup>6</sup> and/or final<sup>7</sup> state effects which determine the photoemission angular distributions. This point is currently under more thorough investigation.

The  $d$  bands of Pt rise sharply to a peak very near  $E_F$ , then show a broad structure extending for about 7 eV. We have calculated the band structure of Pt using Smith's<sup>8</sup> parametrization of the Hodges-Ehrenreich-Lang<sup>9</sup> tight-binding interpolation scheme. Figure 3 shows the calculated total valence-band (VB) density of states and its decomposition into the  $t_{2g}$  and  $e_g$  components. The first VB peak near  $E_F$  is seen to arise in large measure from  $t_{2g}$  orbitals, which, because of high surface sensitivity of the photoemission spectra at  $h\nu = 40.8$  eV,<sup>10</sup> should mainly be located on surface Pt atoms.<sup>11</sup> The dramatic decrease in the intensity of this peak on chemisorption of CO, which is evident in most of the Pt spectra in Fig. 1, indicates the involvement of surface  $t_{2g}$  orbitals in the chemisorption bond(s). A sim-

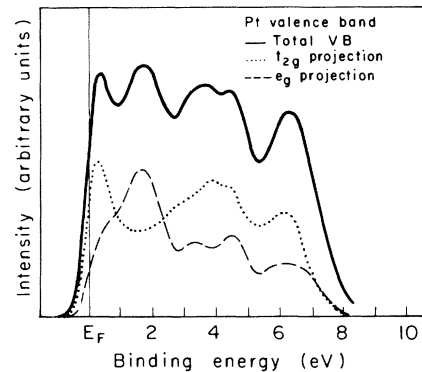


FIG. 3. Total valence-band (VB) density of states and the  $t_{2g}$  and  $e_g$  projections for Pt 5d calculated in a tight-binding interpolation scheme as discussed in the text. The density-of-states histograms were convoluted with a Gaussian of full width at half-maximum = 0.5 eV.

ilar effect has also been observed at higher photon energies.<sup>12</sup>

Neither the location of CO on the substrate nor the exact nature of the CO-substrate bond is yet established. We tend to favor a model in which the C atom lies immediately above a Pt atom, with coordinate covalent ( $\sigma$ ) bonding by the carbon lone-pair electrons, stabilized through back-bonding of  $t_{2g}$  orbitals with the CO  $\pi^*$  orbitals.<sup>13</sup> This is consistent with the spectra, particularly with depletion of the surface  $t_{2g}$  bands, and it is also appealing on chemical grounds (bond-length considerations, for example). Further experimental evidence will be needed, however, before the absolute conformation of the chemisorbed CO-substrate complex is established with certainty.

We would like to thank J. W. Davenport for valuable comments regarding the calculations and for providing unpublished results. One of us (J.S.) would like to thank G. J. Lapeyre for communicating his angle-resolved polarization-dependent results on Ni(001) + CO prior to publication.

\*Work supported by the U. S. Energy Research and Development Administration.

<sup>1</sup>J. W. Davenport, Phys. Rev. Lett. **36**, 945 (1976).

<sup>2</sup>J. Stöhr, G. Apai, P. S. Wehner, F. R. McFeely, R. S. Williams, and D. A. Shirley, Phys. Rev. B (to be published).

<sup>3</sup>T. Gustafsson, E. W. Plummer, D. E. Eastman, and J. L. Freeouf, Solid State Commun. **17**, 391 (1975), and references therein.

<sup>4</sup>J. W. Davenport (private communication) supplied the analytical expression for the cross section and calculated values for  $A(\theta)$ ,  $B(\theta)$ ,  $C(\theta)$ , and  $D(\theta)$ . In case of the CO molecule lying down on the surface, we have as-

sumed a random orientation.

<sup>5</sup>I. P. Batra and P. S. Bagus, *Solid State Commun.* **16**, 1097 (1975).

<sup>6</sup>J. W. Gadzuk, *Phys. Rev. B* **10**, 5030 (1974).

<sup>7</sup>A. Liebsch, *Phys. Rev. B* **13**, 544 (1976).

<sup>8</sup>N. V. Smith, *Phys. Rev. B* **9**, 1369 (1974). Smith's *d*-block parameters were used unchanged. The plane-wave (PW) and *d*-PW hybridization parameters were changed as follows:  $\alpha=0.014$ ,  $V_{200}=0.0082$ ,  $V_{111}=-0.0071$ ,  $B_1=0.4$ ,  $B_2=B_3=1.49$ ,  $\beta=-0.06$ , and a spin-orbit parameter  $\xi=0.038$  Ry.

<sup>9</sup>L. Hodges, H. Ehrenreich, and N. D. Lang, *Phys.*

*Rev.* **152**, 505 (1966).

<sup>10</sup>I. Lindau and W. E. Spicer, *J. Electron Spectrosc. Relat. Phenom.* **3**, 409 (1974); C. R. Brundle, *Surf. Sci.* **48**, 99 (1975).

<sup>11</sup>Modification of the bulk bands at the surface does not change the basic  $t_{2g}$  character of the valence-band peak near  $E_F$ , as shown by M. C. Desjonquères and F. Cyrot-Lackmann, *Solid State Commun.* **18**, 1127 (1976).

<sup>12</sup>G. Apai, P. S. Wehner, J. Stöhr, R. S. Williams, and D. A. Shirley, to be published.

<sup>13</sup>A. E. Morgan and G. A. Somorjai, *J. Chem. Phys.* **51**, 3309 (1969).

## Nonlinear Transport in Tetrathiafulvalene-Tetracyanoquinodimethane (TTF-TCNQ) at Low Temperatures\*

Marshall J. Cohen, P. R. Newman, and A. J. Heeger

*Department of Physics and Laboratory for Research on the Structure of Matter, University of Pennsylvania, Philadelphia, Pennsylvania 19174*

(Received 15 July 1976)

An experimental study of electrical transport phenomena in TTF-TCNQ in the low-temperature ( $T < 4.2$  K) dielectric regime is reported. The current-voltage curves are nonlinear with conductance increasing with increasing voltage. The observed nonlinearity is insensitive to radiation-induced defects at the fraction of a percent level. The data are discussed in terms of electric field depinning of the incommensurate charge-density wave with a critical electric field of approximately  $1.5 \times 10^2$  V/cm.

Extensive studies of the electrical conductivity of TTF-TCNQ have generally focused on two temperature ranges—the one-dimensional metal regime at  $T > 58$  K<sup>1-6</sup> and the region  $38$  K  $< T < 58$  K<sup>7-9</sup> in which a series of three electronic structural transitions have been observed.<sup>10-14</sup> In the dielectric regime below 38 K, the charge-density waves (CDW) are pinned by interchain coupling resulting in a three-dimensional superlattice with  $a_s = 4a$ ,  $b_s = 3.4b$ , and  $c_s = c$  (where  $a$ ,  $b$ , and  $c$  are the lattice parameters of the undistorted structure).<sup>10,12,14,15</sup> However, the unusually large low-frequency dielectric constant<sup>16</sup> and the related low resonance frequency<sup>17</sup> for the coherent pinned phase mode imply relatively weak pinning forces. The question which we have approached experimentally is whether the application of an electric field at low temperatures ( $T \ll 38$  K) can cause the weakly pinned CDW condensate to depin (partially) and thereby become conducting. We report<sup>18</sup> in this Letter the results of an experimental study of nonlinear transport phenomena in TTF-TCNQ at low temperatures.

All measurements of the current-voltage characteristics were carried out on single crystals of TTF-TCNQ with use of the standard four-probe arrangement, with the sample immersed in the liquid-helium bath. Low current levels ( $< 1 \mu\text{A}$ ) were supplied by a simple dividing network using

a battery source and were measured with a Kiethley 160B multimeter. At higher current levels, measurements were carried out in both controlled-current and controlled-voltage configurations with either an electronic measurements C612 constant current supply or a Hewlett-Packard dc power supply in series with a battery. In all cases, the voltage across the sample was measured using a Kiethley 610B electrometer as a high-impedance buffer (gain of one) connected to a Keithley 160 multimeter.

Figure 1 shows the  $I$ - $V$  curves of a crystal of TTF-TCNQ measured along the principal conducting  $b$  axis. The  $I$ - $V$  curves are nonlinear, with the dynamic conductance,  $dI/dV$ , increasing with increasing voltage. As the temperature is lowered, the low-field conductance decreases, but the degree of nonlinearity increases dramatically. The  $I$ - $V$  curves qualitatively appear to be approaching an off-on situation at  $T=0$  K where current is not generated until a "critical" electric field is reached. The degree of nonlinearity is illustrated in detail in the full logarithmic plot. The results shown in Fig. 1 represent current levels as low as  $10^{-10}$  A and power inputs as low as  $10^{-11}$  W. The solid line represents ohmic behavior and is shown for comparison. At the lowest temperatures, the  $I$ - $V$  characteristics of TTF-TCNQ are nonlinear over the entire range meas-